Thermoreflectance spectra of CdO: Band gaps and band-population effects

F. P. Koffyberg
Department of Physics, Brock University, St. Catharines, Ontario, Canada, L2S 3A1
(Received 23 December 1975)

Thermoreflectance spectra of semiconducting CdO single crystals at 100°K with carrier concentrations in the range $(2\text{–}40)\times 10^{18}/\text{cm}^3$ give 2.28 eV for the energy of the direct $\Gamma_{15}-\Gamma_1$ gap. Two indirect gaps are found: $L_3-\Gamma_1$ at 1.09 eV and $\Sigma_3-\Gamma_1$ at 0.84 eV. Theoretical calculations of the shape of the spectrum, taking explicitly into account the band-population effects, are in qualitative agreement with the experimental results. The spectra of sputtered films of CdO differ substantially from single-crystal spectra, suggesting structural differences between films and crystals.

I. INTRODUCTION

In a thermoreflectance experiment one measures the periodic change ΔR of the reflectivity R caused by a periodic modulation ΔT in specimen temperature. The modulated reflectivity spectrum often shows much sharper structure than the direct reflectivity at photon energies corresponding to critical points in the joint-density-of-states function, indicating the position of band gaps.[1,2] The basic modulation mechanism for semiconductors considered in most theoretical discussions so far is the shift of the band gap with temperature. However, for doped semiconductors whose Fermi level lies in the conduction band (cb), a change in temperature will result also in a change in the cb population, with a consequent change in the optical properties. In Sec. II we will discuss the shape of the modulation spectrum when both band gap and cb population are modulated. In Sec. III we will report the experimental thermoreflectance spectra of semiconducting CdO single crystals with varying degrees of cb filling. Band-structure calculations[3–5] for CdO indicate both direct and indirect gaps, but the various calculations do not agree on the exact position of the gaps, nor do previous experiments[6–8] fix their position unambiguously. We will compare theory and experiment in Sec. IV. Finally, in Sec. V we will discuss separately the results for CdO films prepared by sputtering, since they differ considerably from the results obtained on single crystals.

II. THEORY

A. Direct transitions

For an M_0 critical point Batz[2] has derived the following expression for the derivative of the imaginary part of the complex dielectric constant:

$$\frac{d\epsilon_i}{dT} = -C_1(\hbar\omega)^{-2}\eta^{-1/2}F\left(\frac{\chi}{\eta}\right)\frac{dE_g}{dT}\ , \tag{1}$$

where $\chi=\hbar\omega-E_g$, E_g is the direct band gap, η is an empirical temperature-independent damping parameter, F is Batz's universal function, and C_1 is a constant containing the transition probability, which is assumed to be independent of temperature. This expression assumes that the conduction band is empty. Subsequent calculations[9] have taken into account the temperature dependence of η, and resulted in qualitatively different spectral shapes. In our calculation we will neglect any damping, but concentrate on the effect of filling the conduction band. Bottka and Johnson[10] have shown that for a Fermi energy E_F (measured with respect to the bottom of a parabolic conduction band) larger than zero, ϵ_1 is given by

$$\epsilon_i = C_2\,\kappa^{1/2}(\hbar\omega)^{-2}G, \tag{2}$$

where

$$G=(e^D+1)^{-1} \text{ and } D=\frac{E_F-(|\mu|/m_c^*)\chi}{kT}\ ; \tag{3}$$

m_c^* and μ are the conduction-band effective mass and reduced mass, respectively. C_2 is numerically of the same order of magnitude as C_1. We therefore obtain for the temperature derivative of ϵ_i

$$(C_2)^{-1}\frac{d\epsilon_i}{dT} = G(\hbar\omega)^{-2}\chi^{-1/2}\frac{-dE_g}{dT} + BD + B\left(\frac{-dE_F}{dT}-\frac{|\mu|}{m_c^*}\frac{dE_g}{dT}\right)\Big/k, \tag{4}$$

$$B=(\hbar\omega)^{-2}\chi^{1/2}T^{-1}e^D(e^D+1)^{-2}\ . \tag{5}$$

The first term in Eq. (4) comes from the shift of E_g with temperature. It is the counterpart of Eq. (1), but modified by the factor G, which represents the fact that states at the bottom of the cb are filled and therefore do not contribute to ϵ_i. For $\chi \gg E_F$ and $\chi \gg \eta$ Eq. (1) is identical to the first term in Eq. (4), independent of the value of the damping parameter η. The second term represents the changes with temperature in the cb population around the Fermi level. The third term comes from the motion of E_F, relative to E_g, through the band population. The appropriate value of dE_F/dT in this term depends on the car-

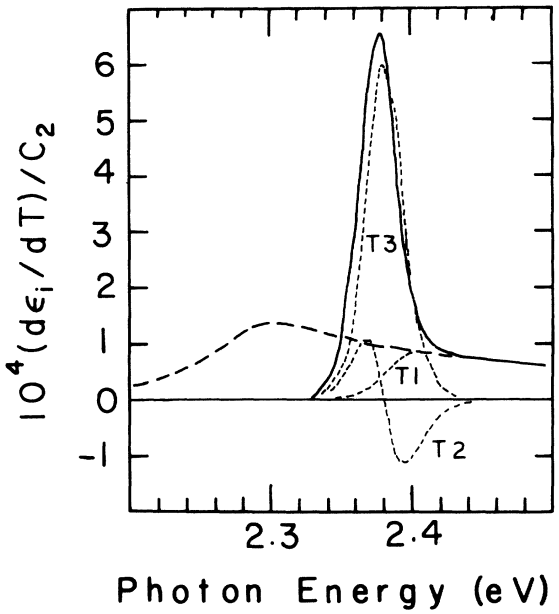

FIG. 1. Derivative of ϵ_i with respect to temperature at a direct gap, calculated without (— —) band-population effects, using Eq. (1), or with (——) band population effects, using Eq. (4). The curves (— — —) marked $T1$, $T2$, and $T3$ are the first, second, and third terms, respectively, in Eq. (4). The following parameters were used: $E_g = 2.28$ eV, $T = 100\,^\circ$K, $|\mu|/m_c^* = 1.0$, $dE_g/dT = -4\times10^{-4}$ eV/° K, $E_F = 0.1$ eV, $dE_F/dT = 0$, and $\eta = 0.04$ eV.

rier concentration n_0 and the effective mass. For CdO, to which we shall apply this theory in Sec. IV, n_0 is temperature independent and the cb population is degenerate. Then dE_F/dT is very small[11] and can be neglected with respect to dE_g/dT. Figure 1 shows the contribution of the three terms in Eq. (4) calculated for parameters appropriate to CdO, their total effect, and Eq. (1) for comparison. The main effect of cb filling is a shift of the maximum from $\hbar\omega \approx E_g$ to $\hbar\omega \approx E_g + E_F$, and the largest contribution comes from the third term. For the parameters used in Fig. 1 the maximum value of $d\epsilon_i/dT$ is much larger than the maximum value predicted by Eq. (1). However, this situation will reverse when both E_F and the damping parameter η in the Batz equation are small: for $(\eta/kT)^{1/2} \lesssim 0.25\,(kT/E_F)^{1/2}\,(m_c^*/|\mu|)$ the values of $d\epsilon_i/dT$ calculated from Eq. (4) become smaller than those calculated from Eq. (1). But for moderately and heavily doped semiconductors the shape and magnitude of the thermomodulated spectrum at a direct transition are clearly influenced by band-population effects.

B. Indirect transitions

The conventional expression for ϵ_i is

$$\epsilon_i = C_3(\hbar\omega)^{-2}N_p\int_0^{\beta}\epsilon^{1/2}(\beta-\epsilon)^{1/2}d\epsilon + C_3(\hbar\omega)^{-2}(N_p+1)\int_0^{\gamma}\epsilon^{1/2}(\gamma-\epsilon)^{1/2}d\epsilon\ , \quad (6)$$

where $N_p = (e^{E_p/kT}-1)^{-1}$ is the phonon occupation factor for phonon energy E_p, and parabolic bands are assumed. The first term represents transitions with phonon absorption ($\beta = \hbar\omega - E_g^* + E_p$), the second term transitions with phonon emission ($\gamma = \hbar\omega - E_g^* - E_p$); E_g^* is the indirect gap. The temperature derivative of ϵ_i, which now contains terms representing both the change in phonon population and the change in E_g^* with temperature, does not show sharp structure at $\hbar\omega = E_g^* \pm E_p$. Rather, $d\epsilon_i/dT$ increases continuously with $\hbar\omega$, and thermomodulated spectra should show at best a weak shoulderlike structure at the band gap.[2]

However, when the conduction band is partially filled, the joint density of states [given by the integrals in Eq. (6)] should be modified by inclusion of a band-occupation factor $(1-f_c)$, where

$$f_c = (1+e^{\epsilon-E_F/kT})^{-1}\ , \quad (7)$$

resulting in

$$\epsilon_i = C_3(\hbar\omega)^{-2}N_p\int_0^{\beta}(1-f_c)\epsilon^{1/2}(\beta-\epsilon)^{1/2}d\epsilon + C_3(\hbar\omega)^{-2}(N_p+1)\int_0^{\gamma}(1-f_c)\epsilon^{1/2}(\gamma-\epsilon)^{1/2}d\epsilon\ , \quad (7a)$$

The temperature dependence of ϵ_i is now given by

$$(C_3)^{-1}\frac{d\epsilon_i}{dT} = (\hbar\omega)^{-2}\frac{E_p}{kT^2}N_p(N_p+1)\left[\tfrac{1}{8}\pi\beta^2 + \tfrac{1}{8}\pi\gamma^2 - I(\beta) - I(\gamma)\right] + (\hbar\omega)^{-2}\frac{-dE_g^*}{dT}\left[\tfrac{1}{4}\pi\beta N_p + \tfrac{1}{4}\pi\gamma(N_p+1) - \tfrac{1}{2}N_pH(\beta) - \tfrac{1}{2}(N_p+1)H(\gamma)\right] - (\hbar\omega)^{-2}\{N_p[K(\beta)+L(\beta)] + (N_p+1)[K(\gamma)+L(\gamma)]\}\ , \quad (8)$$

$$I(\alpha) = \int_0^{\alpha} f_c\,\epsilon^{1/2}(\alpha-\epsilon)^{1/2}d\epsilon\ , \quad (9)$$

$$H(\alpha) = \int_0^{\alpha} f_c\,\epsilon^{1/2}(\alpha-\epsilon)^{-1/2}d\epsilon\ , \quad (10)$$

$$K(\alpha) = \int_0^{\alpha} f_c^2\,\epsilon^{1/2}(\alpha-\epsilon)^{1/2}\frac{\epsilon-E_F}{kT^2}\frac{e^{\epsilon-E_F}}{kT}d\epsilon\ , \quad (11)$$

$$L(\alpha) = \int_0^{\alpha} f_c^2\,\epsilon^{1/2}(\alpha-\epsilon)^{1/2}\frac{e^{\epsilon-E_F}}{kT}\frac{dE_F}{dT}(kT)^{-1}d\epsilon\ . \quad (12)$$

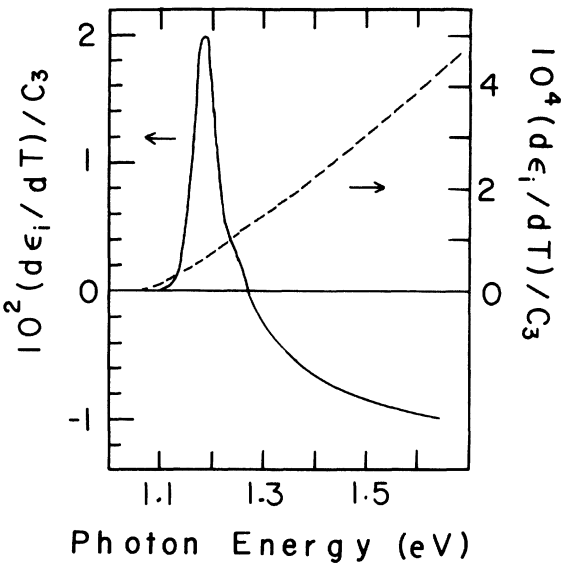

FIG. 2. Derivative of ϵ_i with respect to temperature at an indirect gap, calculated without (– – –) band-population effects (right-hand scale), or with (——) band-population effects [Eq. (8), left-hand scale]. The following parameters were used: $E_g^*=1.06$ eV, $T=100\,^\circ$K, $dE_g^*/dT=-5\times10^{-4}$ eV/°K, $dE_F/dT=0$, $E_F=0.1$ eV, and $E_p=0.016$ eV.

The first term in Eq. (8) represents the contribution of the change in the phonon population with temperature, whereas the second term gives the contribution of the shift of the band gap. Numerical calculations, using parameters appropriate for CdO, show that the third term, representing the change in band population around the Fermi energy, is approximately two orders of magnitude larger than the first two terms. Equation (8) has a maximum (Fig. 2) at $\hbar\omega\approx E_g^*+E_F+1.5E_p$ and is zero at $\hbar\omega\approx E_g^*+2E_F+E_p$. The values of $d\epsilon_i/dT$ for $\hbar\omega\gg E_g^*$ are probably not physically significant, since then the assumption of parabolic bands is likely to break down. The sharp structure and large magnitude of $d\epsilon_i/dT$ around $\hbar\omega\approx E_g^*+E_F$ are in marked contrast to its behavior for transitions into an empty conduction band, for which case the integrals I, H, K, and L are equal to zero. It is clear that band-population effects should make it possible to detect indirect gaps in thermomodulated spectra of moderately doped semiconductors. For such materials direct absorption and reflection spectra rarely show sharp structure at indirect gaps, since the weak absorption shoulders and reflection peaks are overwhelmed by the free carrier absorption.

III. EXPERIMENTAL

Single crystals of CdO, $2\times2\times0.3$ mm,[3] with less than 30 ppm impurities and grown by a vapor transport process,[12] were annealed in oxygen at varying temperatures until their carrier concentration n_0 was constant. Table I gives the annealing temperatures, the O_2 pressure during annealing, n_0, and the value of E_F at 100 °K. The reflecting crystal face was polished with 1-μm diamond, and subsequently etched for a short time in dilute HCl, a procedure which improved drastically the sharpness of the spectra. Thermoreflectance spectra were measured by standard techniques at 300, 200, and 100 °K. The modulating heating current at frequency 1.4 Hz was applied directly to the samples; the modulation amplitude was approximately 2 °C. Figure 3 shows the experimental thermoreflectance spectra for the single crystals at 100 °K; at higher temperatures the spectra are essentially similar, except for a shift of the peaks to longer wavelengths and an increasing broadening of the peaks. The sample E was a 35-μm-thick film on a mi-

TABLE I. Parameters of thermoreflectance samples.

Sample	Annealing temp. (°C)	Annealing pressure (atm)	n_0 (cm^{-3})	E_F (eV) at 100 °K
A	595	1.00	2.35×10^{18}	0.012
B	615	1.00	3.64×10^{18}	0.016
C	727	1.00	1.08×10^{19}	0.043
D	828	0.01	4.25×10^{19}	0.154
E	•••	•••	1.9×10^{18}	0.010

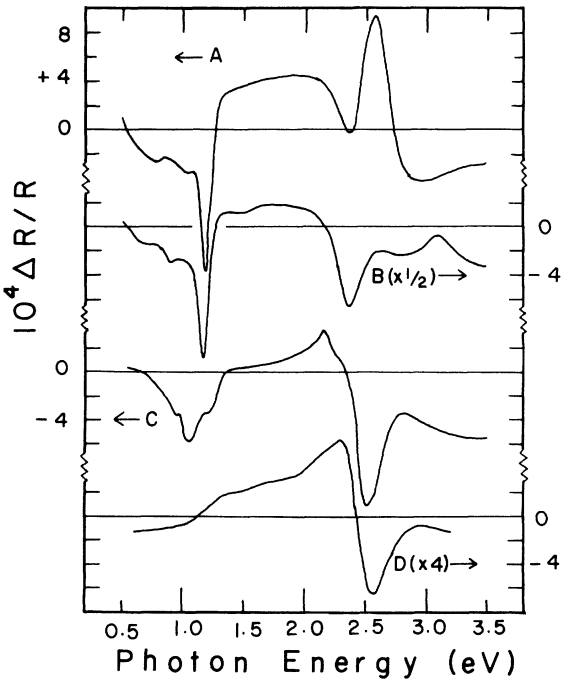

FIG. 3. Thermoreflectance spectra at $T=100\,^\circ$K for the CdO single-crystal samples *A*, *B*, *C*, and *D*.

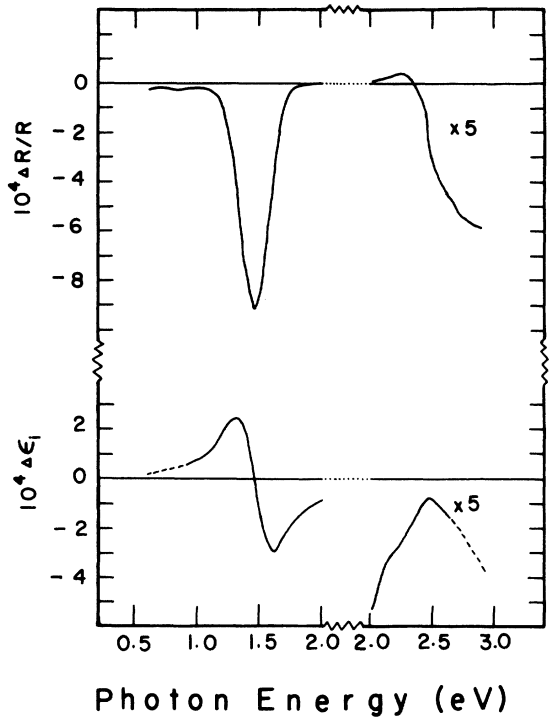

FIG. 4. Thermoreflectance spectrum (upper curves) and $\Delta\epsilon_i$ spectrum (lower curves) at $T=100\,^\circ$K for a sputtered CdO film, sample E.

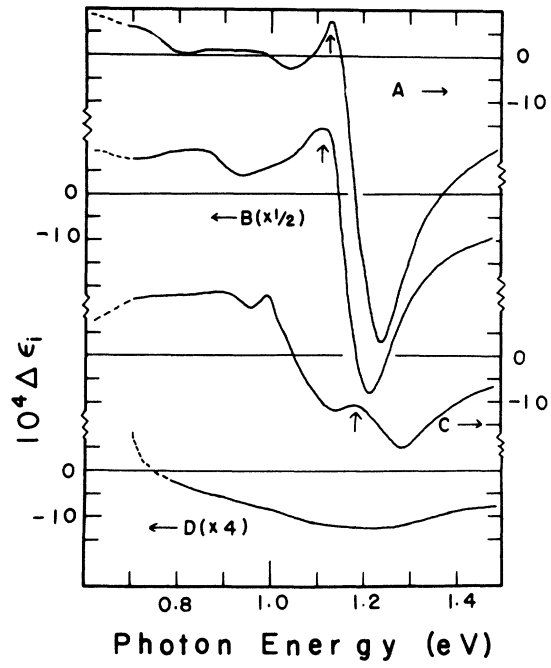

FIG. 5. Change $\Delta\epsilon_i$ of the imaginary part of the dielectric constant in the wavelength region around the indirect gaps, for the CdO single-crystal samples A, B, C, and D at 100 °K.

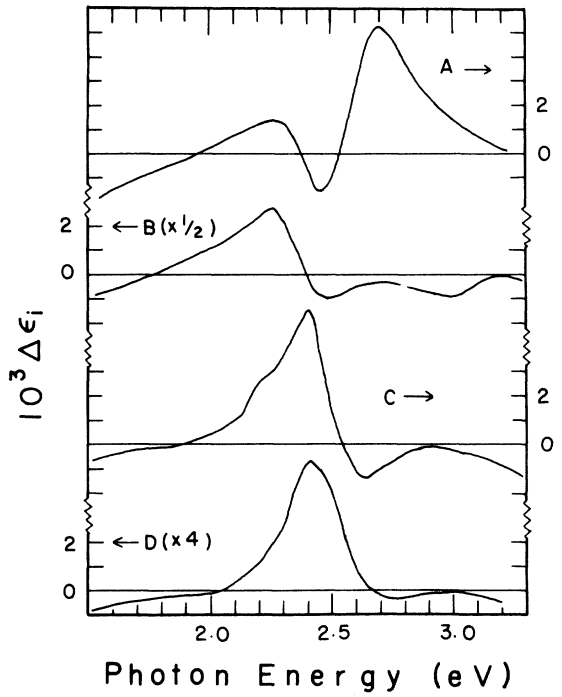

FIG. 6. Change $\Delta\epsilon_i$ of the imaginary part of the dielectric constant in the wavelength region around the direct gap, for the CdO single-crystal samples A, B, C, and D at 100 °K.

croscope cover slip, prepared by rf reactive sputtering of a 99.999% Cd target in dry air. The data for this sample are shown separately in Fig. 4. The existence of different absolute values of $\Delta R/R$ for the various samples is probably not very significant, since $\Delta R/R$ is proportional to the amplitude ΔT of the temperature modulation, and ΔT could have varied by 50% from sample to sample. This does not affect the spectral shape of $\Delta R/R$, however, and there is a systematic change in the thermoreflectance spectrum with changing carrier concentration.

The experimental $\Delta R/R$ spectra were transformed by a Kramers-Kronig analysis into $\Delta\epsilon_i$ spectra; these are shown in Figs. 5 and 6 for the wavelength regions around the indirect and direct gaps, respectively. For an exact Kramers-Kronig integral one needs $\Delta R/R$ values in the range $0<\hbar\omega<\infty$, whereas our data range is $0.5<\hbar\omega<3.5$ eV. This data cutoff gives artificial structure in the spectra of Figs. 5 and 6, and the curves have no physical significance for $\hbar\omega<0.7$ and $\hbar\omega>3.3$ eV.

Finally, we measured the conductivity and Hall coefficient in the range $85<T<300\,^\circ$K. The results agreed within 10% with values obtained previously[12]; specifically, the Hall coefficient was independent of temperature in the measuring range.

IV. DISCUSSION

Cadmium oxide is an n-type semiconductor; its large conductivity is caused by the relatively large concentration of native defects (either cadmium interstitials[13] or oxygen vacancies) acting as donors. Band-structure calculations predict a direct gap of 2.38 eV at the center of the Brillouin zone between the conduction-band minimum of Γ_1 and the valence-band maximum of Γ_{15}. Two indirect gaps have been predicted: between L_3 and Γ_1 at 1.11 eV,[4] or 1.18 eV,[5] and between Σ_4 and Γ_1 at 0.95 eV,[4] or 1.12 eV.[5] Reference 3 gives the indirect gaps as L_3 -Γ_1 at 1.2 eV and Σ_3-Γ_1 at 0.8 eV. The direct gap has been observed in both absorption[14] and reflection[6] spectra, but the analysis of the experimental data is complicated by the presence of the free carrier absorption. This handicap is even more severe in the evaluation of the positions of the indirect gaps from the absorption spectra. Previous investigators have subtracted the (calculated) contribution of the free carrier absorption from the measured spectra; analysis of the difference gives an indirect gap of 1.12 eV at 85 °K for single crystals.[7] Sputtered films of CdO may be prepared with lower carrier concentration than single crystals, diminishing the effect of free carrier absorption. Values of the indirect gaps obtained from sputtered films are[8] 1.35 and[15] 1.2 eV for $L \rightarrow \Gamma$, and 0.55 eV for $\Sigma \rightarrow \Gamma$ at 300 °K.[8] However, we will discuss in Sec. V whether sputtered films give optical data representative of bulk CdO single crystals. Now free carrier absorption is a smooth function of photon energy and only weakly temperature dependent. We expect therefore that it will not produce any structures in the thermoreflectance spectra and we will neglect it in our analysis. We will also neglect exciton effects in these degenerate crystals.

Previous measurements[12,16] have shown that for carrier concentrations $n_0 \gtrsim 10^{18}$ cm^{-3} the donor levels have completely merged with the conduction band, resulting in a degenerate cb population and a Hall coefficient which is independent of temperature. The addition of the donor states makes the cb heavily nonparabolic. In this case the calculation of E_F and its temperature dependence from measured n_0 values depends on how the cb density of states is modified by the added donor states. For our calculation we assume that nearly all added states are at the bottom of the cb, since this model is both mathematically tractable and predicts correctly the electrical properties of CdO at high temperatures.[12] The calculated values of E_F are given in Table I; dE_F/dT was found to be less than 8% of dE_g/dT and was therefore neglected in the calculation of the theoretical $\Delta\epsilon_i$ spectra.

For a quantitative comparison of the theoretical and experimental $\Delta\epsilon_i$ spectra we need to know the appropriate values of the constants C_2 and C_3 in Eqs. (2) and (8). They contain all the wavelength- and temperature-independent parameters, especially the transition probability. Their order of magnitude can be estimated from published spectra[14,7] as $C_2 \approx 10^2$ and $C_3 \approx 10^0$. These values together with Eqs. (2) and (8) predict maximum $\Delta\epsilon_i$ values of one order of magnitude larger than the experimental values. However, of greater importance is that the predicted maximum $\Delta\epsilon_i$ values should be approximately equal in the wavelength regions around the indirect gap ($\hbar\omega \approx 1.1$ eV) and around the direct gap ($\hbar\omega \approx 2.3$ eV). This does agree with the experimental spectra for samples A, B and C, and confirms that band-population effects are the dominant modulation mechanisms.

We ascribe the pronounced structure at $\hbar\omega \approx 1.1$ eV in the experimental spectra to transitions across the indirect L_3-Γ_1 gap. The maxima [marked with arrows in Fig. (5)] should occur at photon energies $\hbar\omega \approx E_g^* + E_F + 1.5E_p$; with[7] $E_p \approx 0.016$ eV this gives an average value for the indirect gap of $E_g^* = 1.09 \pm 0.05$ eV at 100 °K. The sharp drop in the experimental spectra for $\hbar\omega > E_g^* + 2E_F$ probably reflects the nonparabolic shape of both the conduction and valence bands; inspection of the published band structure shows that the valence band is rather asymmetrical at both the L_3 and Σ_3 maxima. The experimental spectra in the indirect-gap region show progressively less structure with increasing n_0; for sample D the indirect gap cannot be detected at all. We do not know whether this general trend is due to nonparabolicity or to more fundamental causes.

The maximum at 1.18 eV for sample C is superimposed on a steady decline in $\Delta\epsilon_i$, which starts from another maximum at 0.99 eV. We ascribe this maximum to the Σ_3-Γ_1 transition; this gives 0.84 eV for this energy gap. The structure in this region of the spectrum for samples A and B is not pronounced enough to extract a E_g^* value from it.

In the wavelength region around the direct gap we identify the pronounced positive peaks in the experimental spectra (Fig. 6) with the theoretically predicted maxima (Fig. 1) at $E_g + E_F$; this gives an average value $E_g = 2.28 \pm 0.05$ eV at 100 °K. The line shapes for samples B, C, and D agree qualitatively with the theory developed in Sec. II, but quantitatively there are two differences: the calculated spectra are much sharper and they do not show negative $\Delta\epsilon_i$ values. Now both the width of the theoretical spectra and the maximum negative value of the second term in Eq. (4) (curve $T2$ in Fig. 1) will increase if the value of the

TABLE II. L_3-Γ_1 gap energy of CdO at 100 °K.

	Material	Method	n_0 at 300 °K (cm^{-3})	E_g^* (eV)
Kocka and Konak, Ref. 7	single crystal	absorption spectra	1.5×10^{19}	1.11
This work	single crystal	thermoreflectance	2.3×10^{18}	1.09
Kohler, Ref. 8	sputtered film	absorption spectra	10^{16}–10^{18}	1.45[a]
This work, sample E	sputtered film	thermoreflectance	1.9×10^{18}	1.47

[a]Calculated from E_g^* at 300 °K using $dE_g^*/dT = -5\times10^{-4}$ eV/° K.

parameter $|\mu|/m_c^*$ is decreased, and significantly better agreement with experiment can be obtained if we set $|\mu|/m_c^*$ equal to 0.25 instead of 1.00. However, we consider such improved agreement fortuitous and the value of $|\mu|/m_c^* = 0.25$ unacceptable for the following reasons: Firstly, it would give experimental E_g values much smaller (for example, 1.8 eV for sample D) than the values obtained from all other spectroscopic determinations. Secondly, it implies a very pronounced valence-band maximum at Γ_{15} with an effective hole mass of $m_v^* \approx 0.05$. This disagrees sharply with the band-structure calculations, which indicate that m_v^* at Γ_{15} should be much larger than the effective electron mass ($0.14m_e$) at Γ_1. The discrepancy between our calculations and experiment may in fact be due to the incorrectness of the assumption that there is a M_0 critical point at the direct gap. The published band structure suggest the possibility of an M_1 or M_2 critical point, but they are not detailed enough to decide the issue. It is possible[10] to calculate numerically the shape of ϵ_i for a M_1 critical point when band-population effects are important, but in the absence of reliable values of the longitudinal and transverse hole masses such a calculation has doubtful validity.

In addition to the $\Delta\epsilon_i$ maximum at $\hbar\omega = 2.28$ eV sample A shows a pronounced peak at $\hbar\omega = 2.69$ eV, indicating that transitions are involved between states whose energy separation is larger by 0.41 eV than the Γ_{15}-Γ_1 gap. Attempts to explain this peak in terms of a Γ_{15} valence band which is split by spin-orbit coupling are not convincing; the estimated[17] value of the splitting is only 0.09 eV. Moreover, invoking spin-orbit splitting leads to the further difficulty of rationalizing the disappearance of the 2.69-eV peak when the population of the cb is increased, as in samples B, C, and D. We have no acceptable interpretation of this peak at present.

Summarizing this section, we may say that the inclusion of band-population effects in the theory allows a qualitatively correct interpretation of the thermoreflectance spectrum of CdO, and gives acceptable values for both the direct and indirect gaps. Better agreement might be obtained if the effects of both the nonparabolicity of the conduction band and the complex shape of the valence band could be explicitly incorporated into the theory.

V. SPUTTERED CdO FILMS

Thin films of CdO may be prepared by reactive dc or rf sputtering of Cd in an oxygen-containing atmosphere; their carrier concentration can be much lower than the limit of $(2\text{–}3)\times10^{18}$ cm^{-3} which can be obtained in single crystals by annealing. We investigated in detail one film, sample E, made by sputtering in dry air; films prepared in a 20%-O_2/80%-argon atmosphere gave similar results. Its impurity content and x-ray diffraction pattern were indistinguishable from those of a crushed single crystal. However, its thermoreflectance spectrum is drastically different (Fig. 4), with an intense minimum at 1.47 eV and a weak, asymmetrical feature at 2.5 eV. The line shapes of both features differ qualitatively from the theoretical shapes for indirect and direct transitions. If we nevertheless assign the 1.47-eV minimum to the L_3-Γ_1 indirect gap, then a comparison with previous results (Table II) shows a clear distinction between gap energies obtained from single crystals and sputtered films.

To account for this distinction one can invoke structural differences or the presence of an impurity band in the films. Now a separate impurity band could form in pure CdO from native donor states when the donor concentration drops below $\sim10^{18}$ cm^{-3}. However, transitions to it should occur at lower photon energies than transitions to the cb, contrary to the experimental results. Moreover, a separate impurity band implies a temperature-dependent Hall coefficient, which was not found for sample E. Therefore we suggest that there are as yet unspecified structural differences between sputtered films and single crystals, resulting in appreciable differences in their optical properties.

ACKNOWLEDGMENTS

I wish to thank N. Koziol and B. Harrison for experimental assistance, E. R. Cowley for helpful discussions, and the National Research Council of Canada for a grant in partial support of this work.

[1]M. Cardona, in *Modulation Spectroscopy* [Suppl. II of *Solid State Physics*, edited by F. Seitz, D. Turnbull, and H. Ehrenreich (Academic, New York, 1969)], Chaps. III and V.
[2]B. Batz, in *Semiconductors and Semimetals*, edited by R. K. Willardson and A. C. Beer (Academic, New York, 1972), Vol. 9, Chap. 4.
[3]K. Maschke and U. Rössler, Phys. Status Solidi 28, 577 (1968).
[4]S. Tewari, Solid State Commun. 12, 437 (1973).
[5]A. Breeze and P. G. Perkins, Solid State Commun. 13, 1031 (1973).
[6]H. Finkenrath and M. von Ortenberg, Z. Angew. Phys. 23, 323 (1967).
[7]J. Kocka and C. Konak, Phys. Status Solidi 43, 731 (1971).
[8]H. Köhler, Solid State Commun. 11, 1687 (1972).
[9]S. Rabii and J. E. Fischer, Surf. Sci. 37, 576 (1973).
[10]N. Bottka and D. L. Johnson, Phys. Rev. B 11, 2969 (1975).
[11]J. Blakemore, *Semiconductor Statistics* (Pergamon, New York, 1962), Chap. 2.
[12]F. P. Koffyberg, J. Solid State Chem. 2, 176 (1970).
[13]F. P. Koffyberg, Solid State Commun. 9, 2187 (1971).
[14]H. Finkenrath, H. Köhler, and M. Lochman, Z. Angew. Phys. 21, 512 (1966).
[15]M. Altwein, H. Finkenrath, C. Konák, J. Stuke, and G. Zimmerer, Phys. Status Solidi 29, 203 (1968).
[16]F. P. Koffyberg, Can. J. Phys. 49, 435 (1971).
[17]Reference 1, p. 70.